25th ABCM International Congress of Mechanical Engineering
October 20-25, 2019, Uberlândia, MG, Brazil

A MODEL OF A LINEAR PERMANENT MAGNET ALTENATOR FOR DESIGN AND OPTIMIZATION: PART I. MODELLING AND VALIDATION

Roger Victor Rodrigues *
Marcelo Braga dos Santos *
Laboratório de Sistemas Mecânicos
rogervrodrigues@gmail.com
marcelo.bragadossantos@ufu.br

Solidônio Rodrigues de Carvalho *
Laboratório de Transferência de Calor e Massa
solidonio@ufu.br

*Universidade Federal de Uberlândia

Abstract. *This paper presents a model of a Linear Permanent Magnet Altenator for design and optimization purposes. It aims to obtain a model without the usual simplifications as, for example, the linearization of the electromagnetic force, and that does not depend on the parameters obtained only via experiments or manufacturers documents. It is shown that the choice of the method for estimate the magnetic field inside the machine was a important step, which leaded to a model with low-computational cost and great precision. The results are validated by comparing the magnetic field distribuition and the flux linkage in the coils with a FEM model. The results also demonstrated that the proposed method is suitable for an optimization algorithm.*

Keywords: *Subdomains model, tubular generator, energy convertion, modelling*

1. INTRODUCTION

Linear Permanent Magnets Alternators (LPMA) are increasingly being proposed as electric generators where prime movers present a natural linear motion, such as free-piston Stirling engines, linear internal combustion engines, and direct wave energy engines. The claimed key advantages of this machine are high power density, high field strength, high efficiency and the fact that no brushes, slip rings or other connections to the translator are necessary (Cawthorne *et al.*, 1999). Futhermore, the use of these type of electrical machine allows obtaining a simpler and compacter equipment with higher efficiency, due to the absence of a mechanism that converts the linear movement to a rotational one (Mikalsen, 2008).

A crucial step in design and optimization of these machines is to calculate the electromagnetic field distribution in their interior. Several techniques exist in the literature to cover these demands. Gysen *et al.* (2010) summarize those methods, relating their advantages and pitfalls. Commonly, the applied method is chosen due to its simplicity and relative small computational time. Unfortunately, the simplifications of these methods can make the estimation of the performance parameters inaccurate. The Finite-Element Method (FEM) can be considered as the most accurate one. But the long computation effort makes it sometimes unsuitable for design and optimization (Gysen *et al.*, 2008).

This paper aims to obtain a numerical model of the LPMA able to provide precise results and fast enough to be solved inside an optimization algorithm in order to obtain the most efficient electrical machine. Considering these goals, a steady-state model would be preferred to meet the required low computational effort. However, due the inherent reciprocal movement of the LPMA, and that is very important to estimate the equipment performance under various excitation forces and electrical loads, a transient model should be used (Boldea and Tutelea, 2009).

The results of the proposed model (i.e. magnetic field and flux linkage in the coils) are validated using a finite element model, which is a precise but very expensive model. The results show that the proposed model meet required precision under a small computational effort. In comparison, the processing time of the chosen method to the FEM was near forty times smaller.

2. MODEL DESCRIPTION

2.1 Holistic model structure

As a transient model, the numerical model primarily aims to describe the translator motion which is governed by Newton's second law. The forces acting upon the linor are mechanical friction forces, the electromagnetic force due to the linear alternator and the excitation force. To accordingly represent these phenomena, a 1 degree of freedom (1 DOF) vibratory system is chosen as model.

The 1 DOF is composed by a moving mass, an elastic suspension, a viscous damper and a LPMA. The mass concentrates the mass of the translator and other elements that may be assembled to it. The viscous damper emulates the mechanical losses in the bearings of the machine. The elastic element represents the stiffness of spring that may be associated with the translator. Finally, the LPMA is a element with which the electromagnetic phenomena are simulated.

Hence, as it is a 1 DOF vibratory system, it should be design to work in ressonance, when low values of excitation forces produces high amplitude of displacement and speed. Thefore, to prevent a catastrophic working condition, the mechanical energy should be dissipated from the 1 DOF vibratory system. In fact, the LPMA works as damper in the system's suspension, so that, transform the mechanical in electrical energy.

Thus, two sub-models were developed in order to determinate numerically the piston motion: the dynamical model and the Linear Permanent Magnet Altenator model.

The model was developed in MatLAB® enviroment. The EDO were solved using the avaliable function *ode45*, which is based on a six-stage, fifth-order, Runge-Kutta method.

The validation of the LPMA model was made by comparing the results with a model solved via FEM.

The input and output variables are shown in Fig. 1.

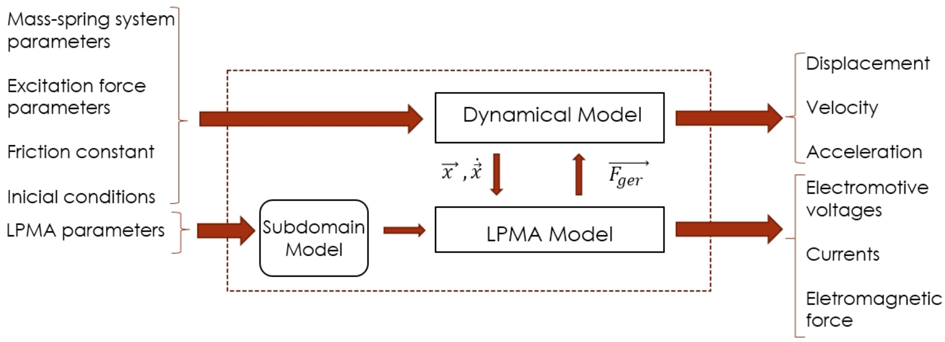

Figure 1. Diagram of the simulation model

2.2 System dynamic model

The dynamical model consists of a mass, a linear spring, the LPMA and a damper, as shown in Fig. 2. The damper was added to model the mechanical losses as ones from viscous and dry friction.

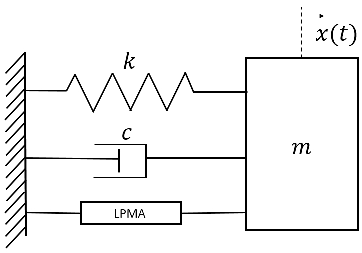

Figure 2. Schematic diagram of the dynamical model.

Equation (1) describes the dynamical behavior of the described model in the state-space formulation.

$$\begin{Bmatrix} \ddot{x}(t) \\ \dot{x}(t) \end{Bmatrix} = \begin{bmatrix} 1/m & 0 \\ 0 & 1/c \end{bmatrix} \left(\begin{bmatrix} c & k \\ -c & 0 \end{bmatrix} \begin{Bmatrix} \dot{x}(t) \\ x(t) \end{Bmatrix} + \begin{Bmatrix} F(t) - F_{ger}(t) \\ 0 \end{Bmatrix} \right) \tag{1}$$

Where m, c and k are the parameters of the mass-spring system – mass, damping and stiffness coefficient, respectively. $F(t)$ and $F_{ger}(t)$ are the excitation and electromagnetic forces.

2.3 Linear Permanent Magnet Altenator Modelling

2.3.1 Subdomains Model

It is often necessary to estimate the rated power, efficiency, magnetic losses and even magnetic vibrations of the electric machines to optimize their design. This estimation relies on the accurate computation of the machine characteristics, such as electromagnetic torque, magnetic losses, and air gap Maxwell forces. All these quantities can be computed if the magnetic field inside the machine is fully determined, meaning the space and time distribution for both radial and tangential components (Gysen *et al.*, 2010; Devillers *et al.*, 2016).

For this purpose, the technique namelly as Subdomain Modeling (SDM) was selected between the different methods available in the scientific literature, due to the advantages it presents. The low computational effort combined with the accuracy of the results – that can be comparable with the solutions obtained via FEM for simple geometries – made SDM an suitable choice for this work. However, the limitations of SDM derive from the inherent assumptions that are made in its procedure, which are described further.

SDM is a semi-analytical method that consists in dividing the problem into physical regions, called subdomains, in which Maxwell governing equations can be solved analytically. Then, Maxwell equations are written in each subdomain for scalar potential or vector potential, from which the flux density is derived. By expressing the boundary conditions of potential and magnetic field continuity at each interface between two subdomains, a linear system of analytical independent equations linking all unknown constants is obtained, Eq. (2) (Devillers *et al.*, 2016).

$$[M]\{X\} = \{S\} \tag{2}$$

Where the matrix $[M]$ is denominated as "topological matrix", and $\{S\}$ the "source vector". Obtaining the value of the constants $\{X\}$ enables to compute the magnetic field's spatial distribution in each subdomain.

The topological matrix and source vector depend on the topology of the electrical equipment and on the region division. There are numerous variants of tubular LPMA, and for the purpose of this work, the selected topology for the LPMA is classified as radial magnetization, internal magnet topology, slotted armature, and three-phase winding. Figure 3 illustrates the mentioned topology.

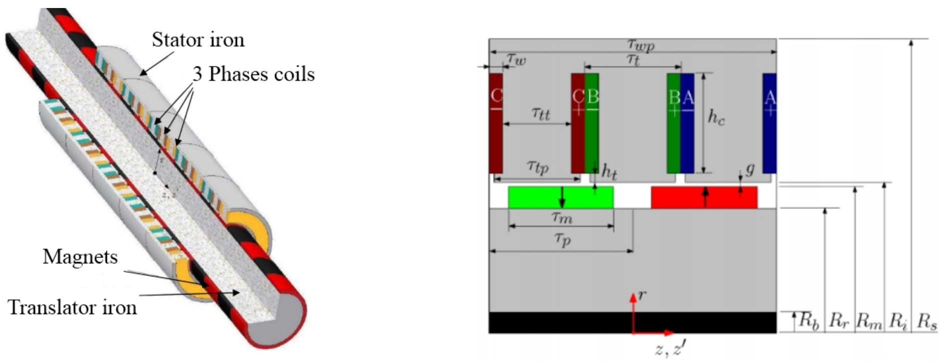

(a) (b)

Figure 3. (a) Topology of the LPMA select for this study. (b) One active part of LPMA with the relevant dimensions. Addapted from Gysen *et al.* (2010).

The formulation proposed by Gysen *et al.* (2010) for the topological matrix and source vector is used in this paper, although the author proposed it for electrical machines used as actuators instead of generators. The division of the chosen topology and the applied boundary conditions used to achieve the mentioned formulation are illustrated in Fig. 4.

The boundary condition is applied according to the material of the delimited regions. A Neumann boundary condition appears at the normal interface between a iron material and a soft-magnetic material. In this condition, the tangential magnetic field strength must be zero. For the continuous boundary condition, the normal component of the magnetic flux density needs to be continuous as well as the tangential component of the magnetic field strength at the delimited boundary. This type of condition is applied between two regions with finite permeability. A combination of Neumann and continuous boundary conditions occurs at an interface between regions which have unequal width and/or unequal offsets, as indicated in Fig. 4. The normal magnetic flux density component of every region should be equal to the normal magnetic field component of air-gap region on the boundary at $r = R_i$. Furthermore, the tangential magnetic field strengh component H_z of the air-gap region must equal the tangential magnetic field strength component of every winding region, on respective boundary, and equal zero elsewhere.

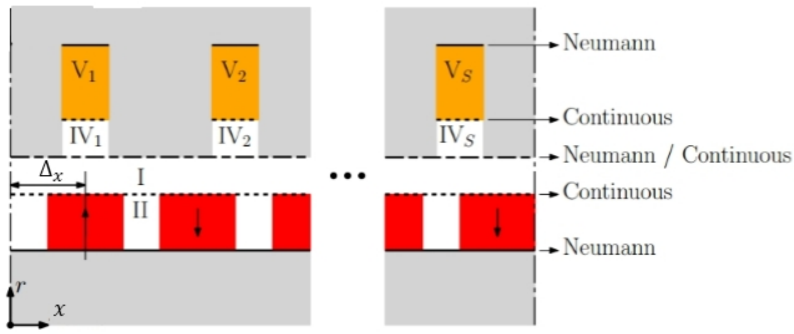

Figure 4. Division in regions and boundary conditions for the choosen topology. Addapted from Gysen *et al.* (2010).

It should be also highlighted that the solution for the magnetic field distribution, obtained via the SDM, in the foregoing machine topology is conditioned on the following assumptions:

1. The axial length of the machine is infinite;
2. The field distribution is axially-symmetric and periodic in the z-direction;
3. The materials properties are linear, homogeneous and isotropic;
4. The permeability of the iron is infinity;
5. The effects due to the Eddy current are neglected;

2.3.2 EMF and Electromagnetic Force calculation

The flux linkage at the coil "$i - th$" due to the magnets for a radially magnetized machine topologies can be obtained as indicated in Eq. (3).

$$\Lambda_{i,pm}(x) = \frac{2\pi}{\tau_o(R_c - R_t)} \int_{R_t}^{R_c} \int_0^{\tau_o} A_\theta^{V,i}(r, \hat{x}, x) \cdot r \cdot dr \cdot d\hat{x} \tag{3}$$

Where $A_\theta^{V,i}(r, \hat{x}, x)$ is the magnetic potential vector at the V_i region, which is function of the constants $\{X\}$, determined by the SDM. One must observe that $\hat{x}$ is the coordinate relative to a fixed reference, and x is the relative displacement between the translator and the stator of the LPMA, as indicated in Fig. 4.

Hence, the electromotive voltage at the *i-th* coil can be calculated with the Eq. (4).

$$e_i(t) = -N_c \frac{d\Lambda_{i,pm}(x)}{dt} = -N_c \frac{d\Lambda_{i,pm}(x)}{dx} \frac{dx}{dt} \tag{4}$$

Where N_c is the number of turns of the coils.

Equation (5) shows the expression by which the electromagnetic force can be calculated.

$$F_{ger} = N_c \cdot N_{pa} \begin{Bmatrix} i_A & i_B & i_C \end{Bmatrix} \frac{d}{dx} \begin{Bmatrix} \Lambda_{A,pm}(x) \\ \Lambda_{B,pm}(x) \\ \Lambda_{C,pm}(x) \end{Bmatrix} \tag{5}$$

Where $\Lambda_{a,pm}(x)$ are the flux linkage at the phase "a" due to the magnets, N_{pa} is the number of active parts of the LPMA and i_a are the instantaneous current for the phase "a".

2.3.3 Electric Circuit Equations

Figure 5 illustrates the schematic diagram of the electrical circuit of the alternator for the phase A, considering that the load of this equipment is a resistor $R_{L,A}$.

In this model, the resistance, the self- and the mutual inductance of the LPMA are considered. Also the possibility to add an inductance $L_{L,A}$ and a capacitor $C_{L,A}$ in the external circuit exists. Therefore, three models were elaborated in this work namelly R-, RL- and RLC model. The intent is to compare the results between the three models and verify the effects of these simplification steps over the results.

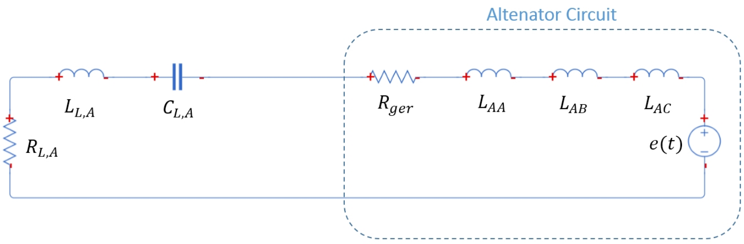

Figure 5. Schematic diagram of the electrical circuit of the alternator for the phase A.

The R model is written considering that both inductance and capacitance of the circuit are neglectable. In that case, the instant current vector is given by Eq. (6).

$$\{i(t)\} = [R_T]^{-1}\{e(t)\} \tag{6}$$

Where $[R_T]$ is $3x3$ diagonal matrix that each element is relative to the resultant resistance for the respective phase circuit. The dimension of the vector $\{i(t)\}$ is equal to the number of phases of the electrical circuit.

The RL model is built considering that only the capacitance of the circuit is null. Then the instantaneous current vector is calculated by solving a EDO system described in Eq. (7).

$$\{\dot{i}(t)\} = -[L_T]^{-1}\left([R_T]\{i(t)\} + \{e(t)\}\right) \tag{7}$$

Where $[L_T]$ is $3x3$ non-diagonal matrix that results from the association of the self- and mutual inductances of the LPMA and the load inductance $L_{L,a}$ of the respective "a" phase circuit.

In the third model – RLC model – all the electrical components shown in the schematic diagram are considered relevant to the dynamical response of the system. The instantaneous current vector is encountered by solving the EDO system in Eq. (8).

$$\begin{Bmatrix} \{\dot{i}(t)\} \\ \{\dot{q}(t)\} \end{Bmatrix} = \begin{bmatrix} [L_T] & [0] \\ [0] & [R_T] \end{bmatrix}^{-1} \left(- \begin{bmatrix} [R_T] & [C_T]^{-1} \\ -[R_T] & [0] \end{bmatrix} \begin{Bmatrix} \{i(t)\} \\ \{q(t)\} \end{Bmatrix} + \begin{Bmatrix} \{e(t)\} \\ \{0\} \end{Bmatrix} \right) \tag{8}$$

Where $[C_T]$ is $3x3$ diagonal matrix that each element is the load capacitance $C_{L,a}$ resistance for the respective "a" phase circuit.

2.4 Equations assembling

The proposed model presents a certain flebility of complexity level, allowing the user to choose the most appropriate for your study. This flexbility rest on the fact that one of three electric circuit models can be selected to applied. For example, if one determines to solve a system using a RL model, then Equation (9) must be solved.

$$\begin{Bmatrix} \ddot{x}(t) \\ \dot{x}(t) \\ \{\dot{i}(t)\} \end{Bmatrix} = \begin{bmatrix} m & 0 & \{0\} \\ 0 & c & \{0\} \\ \{0\} & \{0\} & -[L_T] \end{bmatrix}^{-1} \left(\begin{bmatrix} c & k & \{0\} \\ -c & 0 & \{0\} \\ \{0\} & \{0\} & [R_T] \end{bmatrix} \begin{Bmatrix} \dot{x}(t) \\ x(t) \\ \{i(t)\} \end{Bmatrix} + \begin{Bmatrix} F(t) - F_{ger}(t) \\ 0 \\ \{e(t)\} \end{Bmatrix} \right) \tag{9}$$

Where $F_{ger}(t)$ and $e(t)$ are determined by solving Eq. (5) and Eq. (4), respectively.

In case that one chooses to apply the RLC model, Eq. (7) must be substituted by Eq. (8), resulting in a EDO of four equations, as indicated in the Eq. (10).

$$\begin{Bmatrix} \ddot{x}(t) \\ \dot{x}(t) \\ \{\dot{i}(t)\} \\ \{\dot{q}(t)\} \end{Bmatrix} = \begin{bmatrix} m & 0 & \{0\} & \{0\} \\ 0 & c & \{0\} & \{0\} \\ \{0\} & \{0\} & [L_T] & [0] \\ \{0\} & \{0\} & [0] & [R_T] \end{bmatrix}^{-1} \left(\begin{bmatrix} c & k & \{0\} & \{0\} \\ -c & 0 & \{0\} & \{0\} \\ \{0\} & \{0\} & [-R_T] & -[C_T]^{-1} \\ \{0\} & \{0\} & [R_T] & [0] \end{bmatrix} \begin{Bmatrix} \dot{x}(t) \\ x(t) \\ \{i(t)\} \\ \{q(t)\} \end{Bmatrix} + \begin{Bmatrix} F(t) - F_{ger}(t) \\ 0 \\ \{e(t)\} \\ \{0\} \end{Bmatrix} \right) \tag{10}$$

If the R model is chosen, the dynamic model can be directly solved, considering that the electromotive voltage, the induced current, and therefore the electromagnetic force are fully determined by Equations (4), (6), and (5), respectively.

3. DESIGN

The described model can be used as a reference for a design procedure, independently of the design target, as the electromechanical efficiency or the generated electrical power. The flowchart of the design process is available in Fig. 6.

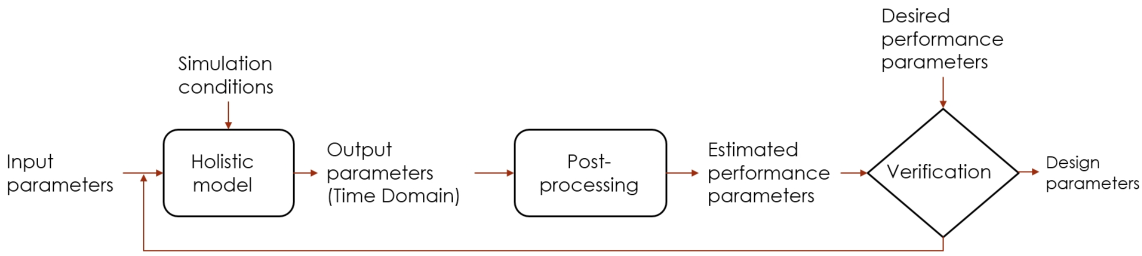

Figure 6. Flowchart of the design procedure of a LPMA

Given the input parameters, as described in Fig. 1, the solution for the output variables in time domain are obtained. If confirmed that the steady-state was achieved, these results are used in a post-processing routine to estimate the performance parameters of the alternator.

In a cycle in the steady-state condition, the mean mechanical power made by the excitation force over the system and the rated electrical power are estimated during one period of oscillation T by the Eq. (11) and (12), respectively.

$$\dot{W}_f = \frac{1}{T}\int_0^T F(t)\cdot x(t)dt \tag{11}$$

$$\dot{W}_{gen} = \frac{1}{T}\int_0^T \sum_{i=1}^{3} e_i(t)\cdot i_i(t)dt \tag{12}$$

Equation (13) is then used to estimate the electromechanical efficiency.

$$\eta_{em} = \frac{\dot{W}_{gen}}{\dot{W}_f} \tag{13}$$

4. RESULTS

4.1 Validation of the Subdomains Model

To validate the results of the method used to estimate the magnetic field inside the electrical machine, a comparison is made with a model solved via FEM. Figure 7 compares the results obtained via SDM and the ones via FEM.

Table 1 shows a quantitative comparison of performances between FEM and SDM. The FEM was implemented in the FEMM environment.

Table 1. Comparison of performance between the Subdomain Model and FEM.
Average results of 5 simulations.

Parameter	Value
Mean Error for B in radial direction (%)	0.639
Mean Error for B in tangential direction (%)	0.128
Mean Error for Flux linkage in Phase A (%)	0.012
Processing time SDM (s)	6.1744
Processing time FEM (s)	247.462

One can observe the obtained error rate are considerably small. The highest value, for the Magnetic field in radial direction, was 0.639%. Furthermore, the processing time using the SDM is near 40 times smaller than one needed for the FEM. The results above are a clear demonstration of the advantages of the SDM, namely the accuracy and the low processing time.

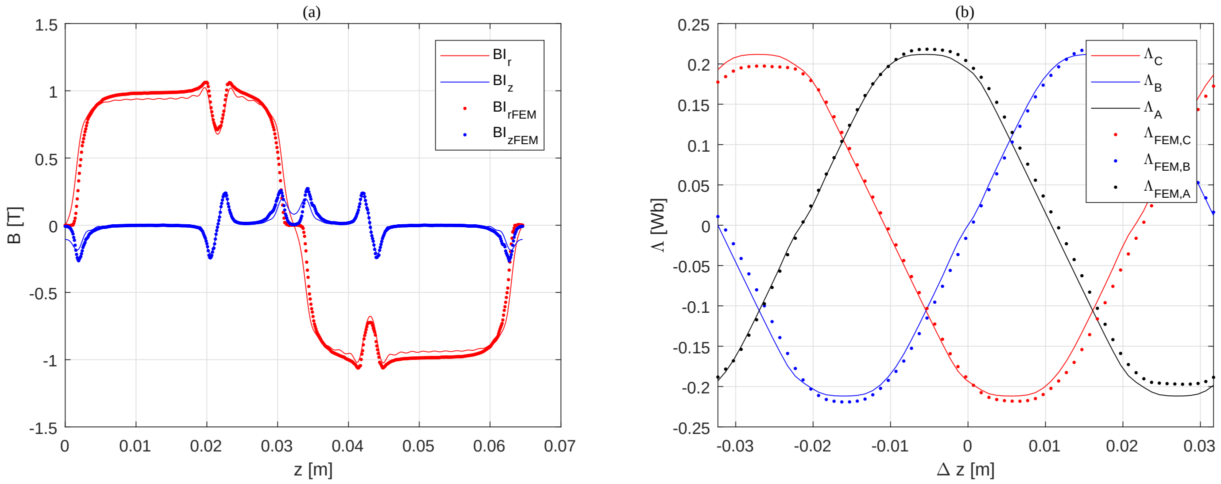

Figure 7. (a) Magnetic field distribution in the air gap due to the magnets. (b) Flux linkage in the coils due to the magnets.

4.2 A design case

The dimensions and parameters of the LPMA used in this example case are available in Table 2. The parameters of the harmonic excitation force were 250 N and 40 Hz for amplitude and frequency, respectively. The parameters of the dynamic system were 5 kg, 315.83 kN/m, and 0 $N \cdot s/m$, for the mass, spring stiffness, and damping coefficient, respectively. The RL model was utilized considering the load resistance equal to 100 Ω and the self- and mutual inductance of the LPMA only.

Table 2. Dimensions and parameters of the LPMA.

Dimension	Value	Description
h_{bi}	7.8 mm	Height of the back iron
h_c	22.5 mm	Height of the coils
h_m	5 mm	Height of the magnets
h_t	2 mm	Height of the teeth tips
g	1 mm	Airgap lenght
N	50	Number of windings
N_p	5	Number of pole-pairs facing the air gap
N_{ph}	3	Number of phases
N_s	15	Number of slots
N_{sp}	5	Number of slots per phase N_s/N_{ph}
R_{ag}	33.8 mm	Mean radius of the air gap
R_b	5 mm	Radius of the aluminium bar
R_i	34.3 mm	Inner radius of the stator
R_m	33.3 mm	Outer radius of the magnets
R_r	28.3 mm	Radius of the iron part of the rotor
R_s	66.6 mm	Outer radius of the stator
τ_m	32.3 mm	Magnet pitch
τ_p	32.3 mm	Pole pitch
τ_t	21.46 mm	Slot pitch
τ_{tt}	15.53 mm	Tooth width
τ_{tp}	19.1 mm	Width of the teeth tips
τ_w	3 mm	Width of the windings
τ_{wp}	64.6 mm	Winding pitch
τ_{ws}	1.18 mm	Width of the current sheets

Figure 8 illustrates the displacement, the instantaneous current and the electromagnetical force obtained at steady-state condition for the study case.

The resultant displacement presents a harmonic characteristic and the instantaneous current curves are typical of the three-phases linear alternators. One can observe that the electromagnetic force presents a strong non-linearity at the moments of higher speed of the translator.

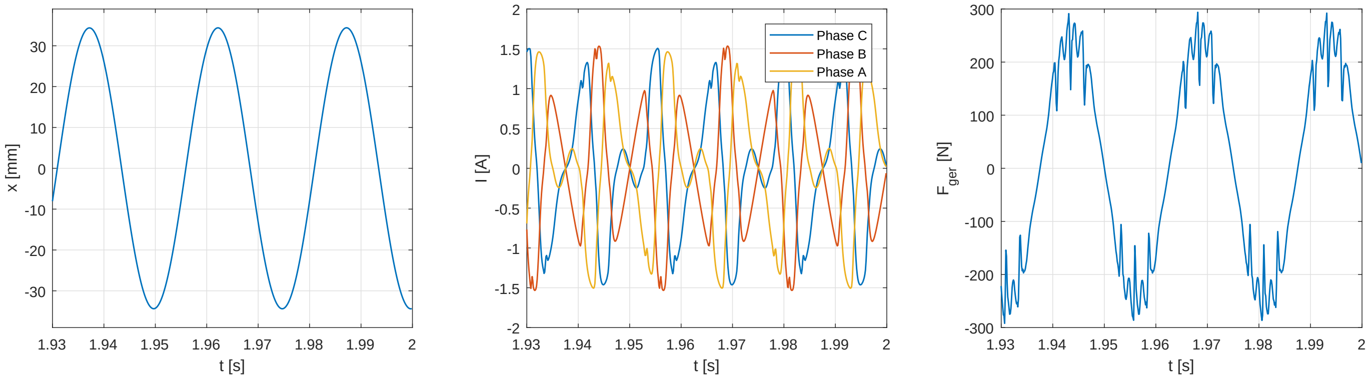

Figure 8. Displacement, instantaneous phase currents and electromagnetical force at steady-state condition.

At the steady-state condition, the achieved frequency is equal to one of the excitation force. Then applied the post-processing routine on the results, using the Eq. (11) to Eq. (13), the estimated rated electrical power was $0.72\ kW$ and the estimated electromechanical efficiency was $87.35\ \%$.

Frequency domain analysis would allow observing how the energy, delivered to the system, would be spread through the frequency spectrum. Figure 9 shows the magnitude of the displacement, velocity and electromagnetic force in the frequency domain, obtained with the Fast Fourier Transform.

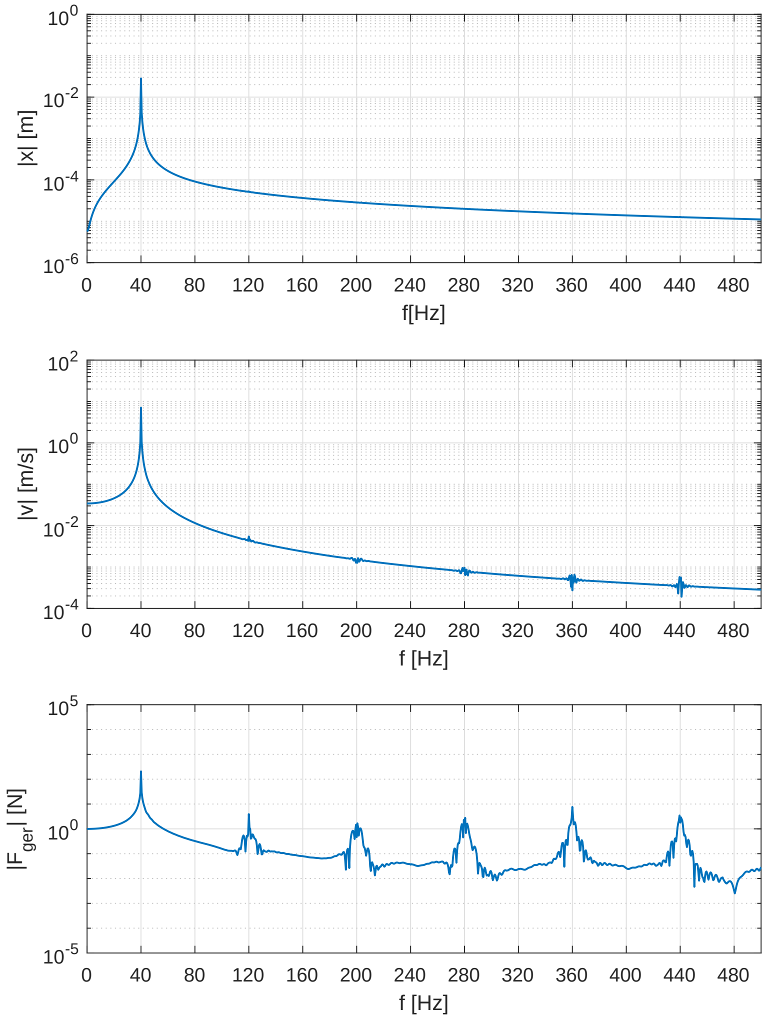

Figure 9. Amplitude of the displacement, velocity and electromagnetical force in frequency domain at steady-state condition.

One can observe that the displacement and velocity presents a similar behavior when compared with results that would be obtained for 1 d.o.f. systems with viscous damper. However, the electromechanical force graph shows the presence of several harmonics. Due to the fact that the flux linkage in the coils flattens towards the excursion of the translator, as shown in Fig. 7(b), the presence of the harmonics may occur in the electromotive voltage $e(t)$ and in the induced currents $i(t)$.Since the electromechanical force is the product of electromotive voltage and the induced current, it would be reasonable that the referred harmonics also be present, as one can observe in the figure above.

5. Conclusions

Several techniques exist in the literature to calculate the electromagnetic field distribution in the interior of an electrical generator, each one with their advantages and pitfalls. For a design and optimization stage, commonly the applied method is chosen due to its small computation effort, even if that leads to less inacurate results. Then this paper proposes a model of a Linear Permanent Magnet Alternator for design and optimization purposes, which meets the precision under a low computation time.

A detailed description of the model was described. To estimate the variables of the magnetical domain, the Subdomain Modelling Method was selected due to the advantages it presents. Three models of electric circuit were elaborated, considering the possibility of using an inductance or capacitance elements associated to the circuit.

To validate the proposed model, the results for magnetic field and flux linkage are compared with the ones obtained via a finite element model. For the magnetic field estimation in the radial direction, the mean error was $0.639\ \%$, while for the flux linkage in phase A the mean error was $0.012\ \%$. Furthermore, the processing time for estimating those variables was nearly 40 times smaller than the one needed for the FEM. Then, the results demonstrated that the proposed method is suitable for an optimization algorithm.

6. ACKNOWLEDGEMENTS

The authors gratefully acknowledge financial support from the CAPES/CNPq.

7. REFERENCES

Boldea, I. and Tutelea, L.N., 2009. *Electric Machines: Steady State, Transients, and Design with MATLAB®*. CRC press.

Cawthorne, W.R., Famouri, P., Chen, J., Clark, N.N., McDaniel, T.I., Atkinson, R.J., Nandkumar, S., Atkinson, C.M. and Petreanu, S., 1999. "Development of a linear alternator-engine for hybrid electric vehicle applications". *IEEE transactions on vehicular technology*, Vol. 48, No. 6, pp. 1797–1802.

Devillers, E., Le Besnerais, J., Lubin, T., Hecquet, M. and Lecointe, J.P., 2016. "A review of subdomain modeling techniques in electrical machines: performances and applications". In *Electrical Machines (ICEM), 2016 XXII International Conference on*. IEEE, pp. 86–92.

Gysen, B., Lomonova, E., Paulides, J. and Vandenput, A., 2008. "Analytical and numerical techniques for solving laplace and poisson equations in a tubular permanent-magnet actuator: Part i. semi-analytical framework". *IEEE Transactions on Magnetics*, Vol. 44, No. 7, pp. 1751–1760.

Gysen, B., Meessen, K., Paulides, J. and Lomonova, E., 2010. "General formulation of the electromagnetic field distribution in machines and devices using fourier analysis". *IEEE Transactions on Magnetics*, Vol. 46, No. 1, pp. 39–52.

Mikalsen, R., 2008. *An investigation into the free-piston engine concept and its potential for high efficiency and low emissions power generation*. Ph.D. thesis, Newcastle University.

8. RESPONSIBILITY NOTICE

The authors are the only responsible for the printed material included in this paper.